Fatigue Crack Initiation and Propagation in Butt Joint Welds of an Ultrahigh-Strength Steel

Formulas proposed for predicting fatigue crack intitation and propagation agree well with experimental data

BY B. LÜ, X. ZHENG AND D. LI

ABSTRACT. In this paper, the fatigue crack initiation (FCI) from notches and fatigue crack propagation (FCP) in different zones of welds in butt joints of 30CrMnSiNi2A steel were investigated. General formulas for the FCI life and the FCP rate of the welds are examined, and an approach to predicting the FCI life is offered. Our research indicates that the postweld isothermal quenching treatment improves both the microstructure and fatigue resistance of the welds. Little difference is found in the FCI resistance of the base metal, weld metal and weld interface, although the microstructural effect on the FCP rate is observed. In the near-threshold region, the FCP rates of the weld interface are higher than those of the base metal but lower than those of the weld metal. The discontinuities on the notch surface have a detrimental influence on the FCI resistance of the welds investigated. The results further indicate that, in order to predict the fatigue life of the welded structures accurately, the test results of FCI life and FCP rate should be properly selected according to the FCI location and FCP path in the structures.

Introduction

The fatigue failure of a welded structure consists of two phases: fatigue crack initiation(FCI) phase and fatigue crack propagation (FCP) phase (Refs. 1, 2).

B. LÜ, S. ZHENG and D. LI are with the Department of Materials Science and Engineering, Northwestern Polytechnical University, Xi'an, Shaanxi Province, People's Republic of China.

$$N_f = N_i + N_p \qquad (1)$$

Depending on the structural details, the crack may initiate at the weld toe, the weld discontinuities or at other locations of stress concentration. The crack then propagates into the weld metal or the base metal (Refs. 1, 3, 4). The role of FCI life and FCP life depends upon the welding quality and the structural details (Ref. 3). For an ultrahigh-strength steel component, the critical crack size to induce the final fracture is rather small because of the lower ratio of fracture toughness/yield strength. Therefore, the FCI life should not be overlooked in the life prediction if there exists no crack-like discontinuity in the component (Refs. 3, 4).

A weldment can be considered as a notched component because it usually contains stress concentration. The stress cycles that initiate a critical crack from notches can be predicted by the local stress-strain approach (Refs. 2, 5, 6). According to the basic assumption of this approach, the stress cycles needed to initiate a fatigue crack at the notch tip are equal to the life of a smooth specimen under cyclic strain control if this specimen has the same stress/strain history as the material ahead of the notch (Refs. 5, 6). So the fatigue notch factor, K_f, cyclic stress-strain curve, and fatigue life under cyclic strain control for the material at the notch tip should be predetermined before the FCI life prediction. However, it is rather difficult to measure accurately such data for the material at some FCI locations, such as the weld toe. The effects of various factors on the accuracy of the local stress-strain approach has been summarized in Ref. 7. Forman (Ref. 8) first measured the FCI life of materials with a notched specimen and found it correlated with the maximum elastic stress range at the notch root, $\Delta\sigma_{max}$, whereas $\Delta\sigma_{max}$ is proportional to the fracture mechanics parameter $\Delta K/\sqrt{\rho}$.

$$\Delta\sigma_{max} = K_t \Delta S = \frac{2}{\sqrt{\pi}} \frac{\Delta K}{\sqrt{\rho}} \qquad (2)$$

where K_t is the stress concentration factor, ΔS is the nominal stress range, ΔK is the apparent stress intensity factor and ρ is the radius of the notch tip. It is convenient to determine the FCI life of materials in different zones of welds by using notched specimens. The FCI life data so obtained can be directly used in the life prediction of engineered structures.

The FCP life of welds depends on the growth rate of the crack from its original size to the critical size, and it can be pre-

KEY WORDS

Fatigue Crack
Crack Initiation
Crack Propagation
Welded Structure
High Strength Steel
Butt Joint Weld
Microstructure
Postweld Treatment
Fatigue Resistance
Weld Geometry

Table 1 — Tensile Properties of 30CrMnSiNi2A Steel

σ_b MPa	$\sigma_{0.2}$ MPa	δ %	ψ %	σ_f MPa	ϵ_f	n	E GPa
1584	1324	13.6	50.8	2147	0.71	0.082	205.8

dicted by means of a fracture mechanics approach (Refs. 1, 9, 10). Paris's law is often used for the FCP rate expression in a welded component (Refs. 9, 10):

$$\frac{da}{dN} = C(\Delta K)^m \tag{3}$$

It was found that the mechanism to form a fatigue crack of 1 to 2-mm (0.04–0.08-in.) depth at the weld toe surface occupies about 55 to 90% in the total life of groove or fillet welds (Refs. 1, 11). This indicates that the major part of the FCP life of a welded component is often spent in near-threshold crack growth. Paris's law, however, cannot be used to predict the FCP rates in the near-threshold region. Obviously, a formula that gives a good prediction of the FCP rates in the near-threshold region is useful in the damage tolerance design of welded structures (Refs. 1, 12).

In this paper, the FCI life of the base metal, weld metal and weld interface of butt joint welds on an ultrahigh-strength steel (30CrMnSiNi2A) are experimentally investigated. The test data are analyzed with the models of FCI (Ref. 13) and FCP (Ref. 14) developed by one of the authors, and formulas for the FCI life and FCP rates are given. These expressions have been utilized to predict the fatigue life of the welded specimens (Ref. 4).

Material and Testing Procedure

Material and Specimen

The test specimens were strips of 30CrMnSiNi2A steel forgings. Their composition in wt-% is 0.30C, 1.09Cr, 1.16Mn, 1.03Si, 1.51Ni, 0.09Cu, 0.04S, 0.01P and balance Fe. The tensile properties are presented in Table 1, where σ_b is the ultimate tensile strength. $\sigma_{0.2}$ is the yield strength, δ is the elongation using a gauge of 25 mm (1 in.) (5 X diameter), ψ is the reduction in area, σ_f is the fracture strength, ε_f is the fracture ductility, n is the strain hardening exponent and E is Young's modulus. The strips were welded with the shielded metal arc process. In order to investigate the crack initiation and propagation in the weld metal and the weld interface, two types of welded specimens were used — Fig. 1. Single-V-groove weld specimens were utilized in the fatigue tests of the weld metal, and double-bevel-groove weld specimens were used for the tests on the weld interface. The rough-machined specimens were austenized at 900°C (1652°F), isothermal quenched and held in a salt bath of 250°C (482°F) for one hour, and then they were tempered for three hours at 250°C.

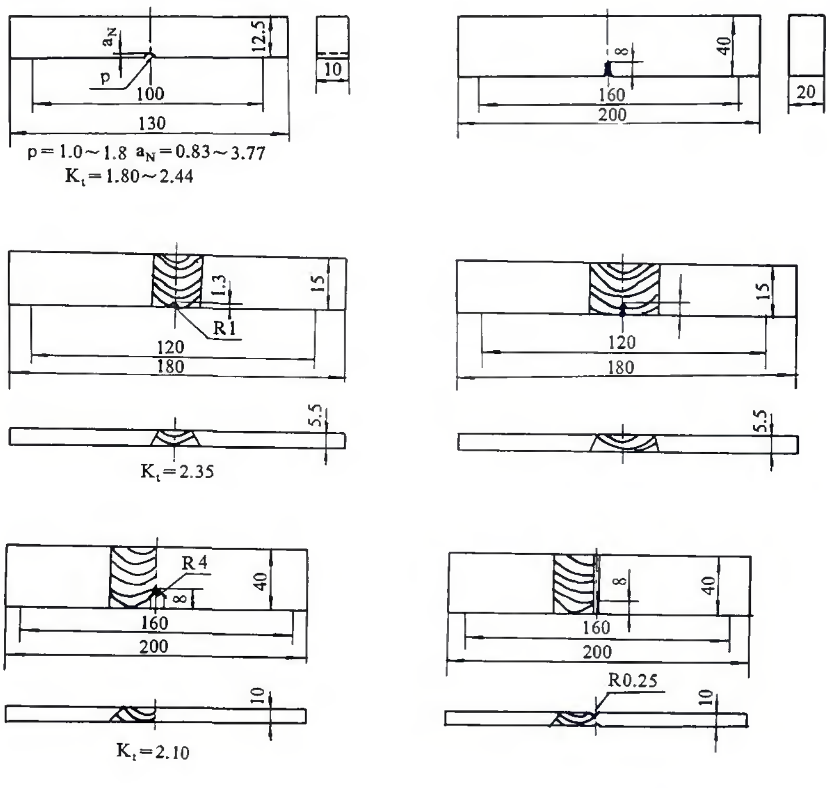

Fig. 1 — Specimen geometries. Left — For FCI tests; right — for FCP tests.

Notched three-point bend specimens (Fig. 1) were used to determine the FCI life. The stress concentration factors of the specimens, K_t, are in the range of 1.80 to 2.44, which are estimated from Ref. 12. The nominal stress range ΔS was calculated from material mechanics theory (Ref. 12):

$$\Delta S = \frac{3\Delta PL}{2B(W - a_n)^2} \tag{4}$$

where ΔP is the cyclic load range, a_n is the notch depth, and L, B and W are the span, thickness and width of the specimens, respectively.

The notched three-point bend specimens (Fig. 1) were also used to measure the FCP rates. In order to control the crack propagation along the weld interface, the specimens were notched with side grooves along the crack growth path. These specimens were used to measure the FCP rates of the weld interface. The stress intensity range of the side-grooved specimens, ΔK, was calculated as follows (Ref. 16):

$$\Delta K = \frac{\Delta P}{\sqrt{(B_n BW)}} f\left(\frac{a}{W}\right) \tag{5}$$

where B_n is the thickness at the root of the side grooves, *a* is crack length and f(a/W) is the same as that of normal three-point-bend specimens.

All specimens were machined in the L-T orientation. Before testing, the specimens were slightly polished to facilitate crack observation and measurement.

Fatigue Tests

The FCI tests were accomplished on an Amsler 422-type high-frequency fatigue machine at frequencies of approximately 60 to 90 Hz, depending on the geometries of the specimens. The stress ratios, R, were in the range of 0.2 to 0.75. In the present study, the FCI life was defined as the stress cycles needed to initiate a 0.25-mm crack at the notch tip. The FCI threshold, denoted as $(\Delta\sigma_{eqv})_{thE}$, was experimentally determined by using a staircase procedure with a specific FCI life of 5 X 10^6 cycles. The FCP tests were carried out on a Mayes-type electroservo hydraulic machine at frequencies of 4 to 15 Hz. The stress ratios R were 0.2, 0.4 and 0.6. The crack length was monitored and measured with two traveling microscopes of 30X magnification fixed on both sides of the specimen. The other procedure details are given in Ref. 17.

Results and Discussion

FCI Test Results

Theoretical analysis (Ref. 10) and experimental results (Refs.1, 3, 4, 17, 18) show that the stress cycles needed to initiate a crack of 0.25-mm (0.10-in.) depth at the notch tip can be formulated as follows:

$$N_i = C\left[\Delta\sigma_{eqv}^{\frac{2}{1+n}} - \left(\Delta\sigma_{eqv}\right)_{th}^{\frac{2}{1+n}}\right]^{-2} \qquad (6)$$

where $\Delta\sigma_{eqv}$ is the equivalent stress amplitude,

$$\Delta\sigma_{eqv} = \sqrt{\frac{1}{2(1-R)}}K_t\Delta S \qquad (7)$$

C is the FCI resistance coefficient and $(\Delta\sigma_{eqv})_{th}$ is the FCI threshold. Incorporating Equation 2 into Equation 7, we have:

$$\Delta\sigma_{eqv} = \sqrt{\frac{2}{\pi(1-R)}}\frac{\Delta K}{\sqrt{\rho}} \qquad (8)$$

when R is held constant, $\Delta\sigma_{eqv}$ and $\Delta K/\sqrt{\rho}$ are equivalent. The research conducted in the authors' laboratory (Ref. 19) indicates that an equal $\Delta\sigma_{eqv}$ will produce an equal local strain range at the notch tip. Consequently, the equivalent stress amplitude can present the effect of stress ratio on the FCI life. The values for C and $(\Delta\sigma_{eqv})_{th}$ can be determined from the test data of FCI life by means of the regression analysis method given in Ref. 13. The values of C and $(\Delta\sigma_{eqv})_{th}$ of the base metal and welded metal so obtained are listed in Table 2. The same analysis does not apply to the test data of the weld interface because only a few specimens were tested in this study. Figure 2 presents the least-square fits to the test data. Incorporating the values of C and $(\Delta\sigma_{eqv})_{th}$ into Equation 6, we have the expressions of the FCI life for the base metal

$$N_i = 6.49\times 10^{15}\left[\Delta\sigma_{eqv}^{1.85} - 649^{1.85}\right]^{-2} \qquad (9a)$$

and for the weld metal

$$N_i = 6.25\times 10^{15}\left[\Delta\sigma_{eqv}^{1.85} - 639^{1.85}\right]^{-2} \qquad (9b)$$

The FCI Threshold

The FCI threshold determined experimentally, $(\Delta\sigma_{eqv})_{thE}$, is the equivalent to the stress amplitude at or below which no fatigue crack initiates at the notch tip after 5 X 10^6 stress cycles. The values of $(\Delta\sigma_{eqv})_{thE}$ thus determined are 810 MPa (117.5 ksi) for the base metal and 766 MPa (111.1 ksi) for the weld metal.

In order to investigate the physical nature of the FCI threshold, the specimens were tested again at higher equivalent stress amplitudes after they had been subjected to more than 5 X 10^6 cycles at the stress level of the FCI threshold. The results in Fig. 2 show that the prior stress cycling at the FCI threshold has no effect on the FCI life. The same phenomenon was also found in a low-alloy steel (0.16C, 1.53Mn, 0.26Si, 0.16V, 0.024N, Fe bal) (Ref. 18) and LY12CZ aluminum alloy (equivalent to 2024-T3) (Ref. 13). This indicates that the FCI threshold is also the fatigue damage threshold and that the stress cycling at or below the threshold produces no damage in notched elements.

Discussion on the FCI Test Results

Effect of Microstructure

The micrographs in Fig. 3 indicate that, after the isothermal quenching treatment, the metastable constituents in the weld metal and the heat-affected

Table 2 — Analysis Results of the FCI Life Test Data

	C		$(\Delta\sigma_{eqv})_{th}$ MPa		r[a]	s[b]
Material	exp.	pred.	exp.	pred.		
Base metal	6.47 × 10^{15}	2.28 × 10^{15}	649	665	−0.777	0.413
Weld metal[b]	6.25 × 10^{15}	2.28 × 10^{15}	639		−0.855	0.359
All data[b]	6.48 × 10^{15}	2.28 × 10^{15}	648		−0.836	0.371

(a) r—the correlation coefficient; s—the standard deviation.
(b) In the regression analysis the strain hardening exponent of the base metal was used.

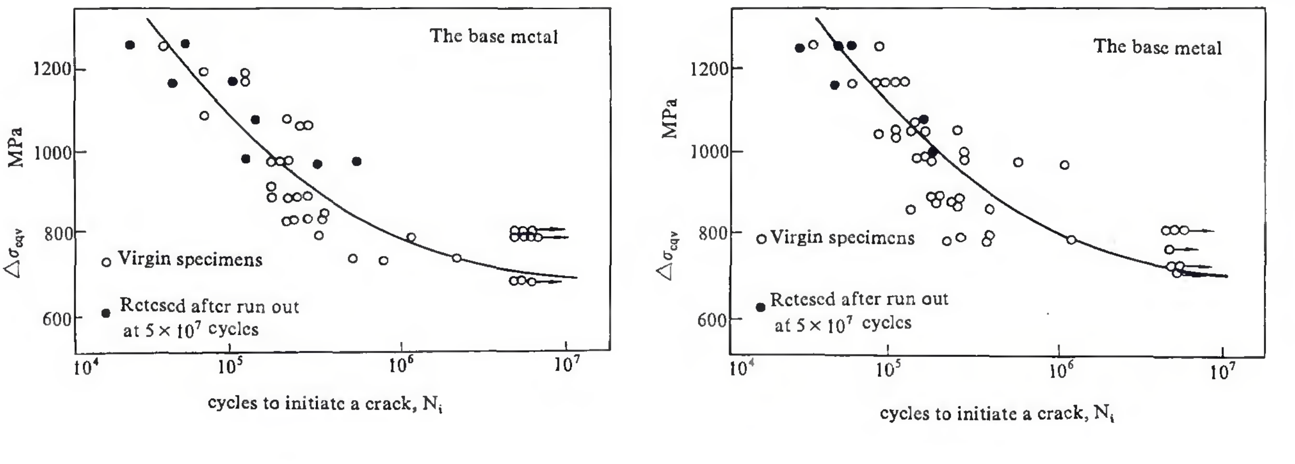

Fig. 2 — The test results and the least-square fit curves. A — Base metal; B — weld metal.

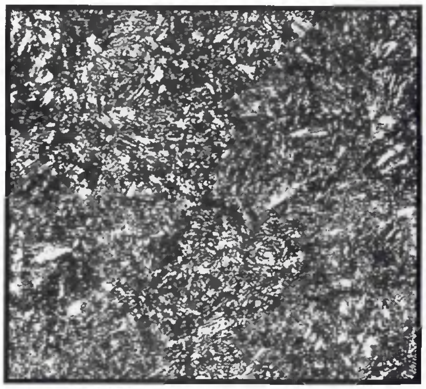

A

Fig. 3 — Microstructures of the groove welds on 30CrMnSiNi2A steel (light micrographs: 3% nitric alcohol etchant). A — Base metal; B — weld metal; C — weld interface; D — HAZ.

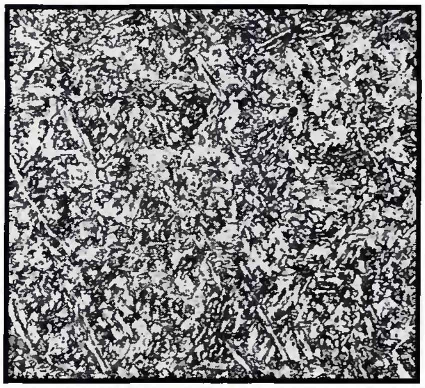

B

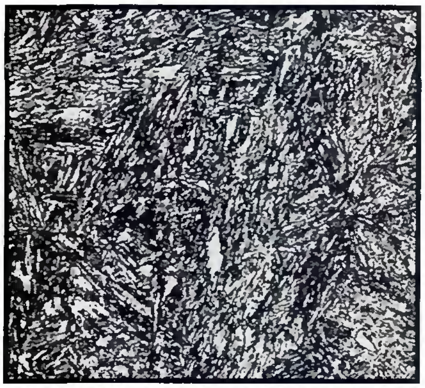

C

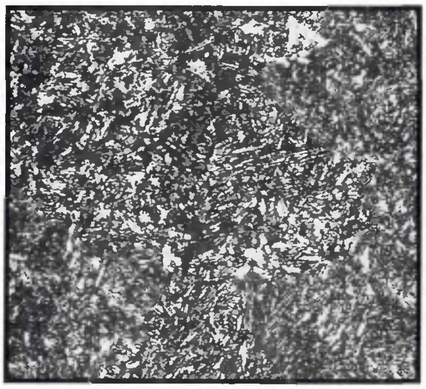

D

zone (HAZ) dissolve and both the microstructure and grain size are refined. The grain sizes in the base metal, weld metal and HAZ are nearly the same, corresponding to ASTM standard No. 9. It has been shown (Refs. 20, 21) that the microstructure in the base metal and the HAZ is a mixture of lath martensite, lower bainite and retained austenite, but the microstructure of the weld metal (18Cr-Mo) is a mixture of lath martensite and granular bainite. Although the microstructure is different, little difference is found in the FCI resistance of the base metal, weld metal and weld interface — Fig. 4. One reason for this is probably that the postweld heat treatment refines the microstructure and removes the harmful residual stresses formed during welding. Since the morphology of the microstructure of the HAZ is almost the same as that of the base metal, the FCI resistance in the HAZ and the base metal may be considered to be approximately the same. By processing all the test data obtained in the different zones by means of the regression analysis method mentioned previously, we obtain the general expression for FCI life in groove welds on 30Cr-Mn-Si-Ni-2A steel as follows:

$$N_i = 6.48 \times 10^{15}\left[\Delta\sigma_{eqv}^{\ 1.85} - 648^{1.85}\right]^{-2} \qquad (10)$$

The FCI life curve given by Equation 10 and the test data are compared in Fig. 4.

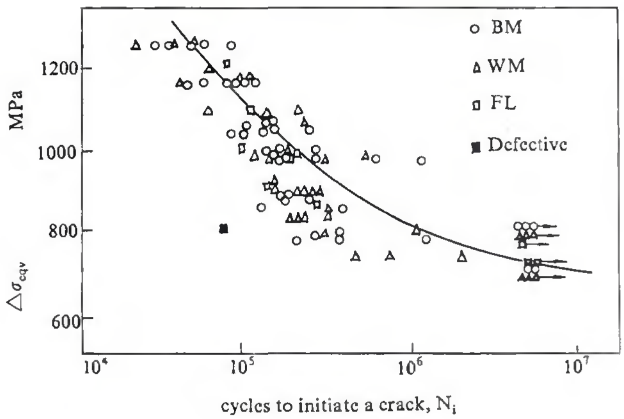

Fig. 4 — The test data of the FCI life in different zones and the least-squares fit curve of the groove welds on 30CrMnSiNi2A steel. BM: base metal; WM: weld metal; FL: weld interface; Defective: welded specimen with cavities at notch tip.

Effects of Weld Discontinuities

Depending upon the effect on the FCI life, welding discontinuities are divided into two types: crack-like and noncrack-like (Ref. 3). A crack-like discontinuity, such as incomplete fusion, acts as a crack and propagates immediately as long as the cyclic stress intensity range, ΔK, is higher than the FCP threshold, ΔK_{th} (Refs.3, 4). However, a noncrack-like discontinuity, such as a cavity, acts as a notch, and its effect on the FCI depends upon the stress concentration at the root of the discontinuity (Refs. 1, 3, 4). In this investigation, only cavities were found in the weld specimens. Figure 4 indicates that if cavities are present at the root of the surface notch, the

FCI life will decrease remarkably because the cavities increase the stress concentration in the specimens. It was also found in the tests that a crack in one of the welded specimens initiated from cavities outside of the notch. These cavities have a tendency to congregate in close proximity. The radius of a single cavity is about 0.2 to 0.5 mm (0.007–0.019 in.). The FCI life of the specimen with the discontinuities was about the same as the life of a notched specimen without discontinuities if their nominal stress was identical. This indicates that the stress concentration factor at the tip of the cavities is slightly greater than 2.36, the value of K_t at the notch root. It agrees with the analytical results in Ref. 22.

FCI Resistance Coefficient C

The FCI coefficient C is a material constant depending upon the FCI mechanism and the tensile properties (Refs. 13, 17, 23). For the isothermal quenched 30CrMnSiNi2A steel, there is retained austenite (about 10% in wt-%) in the interstices of the lath martensite. During cyclic deformation, the plastic strain tends to concentrate in the softer austenite due to the sliding of the lath martensite, so that the fatigue crack is likely to initiate in the retained austenite when the cyclic stress level is higher (Ref. 24). In this case, the value of C can be approximately estimated as follows (Ref. 12):

$$C = 0.25(0.1E)^{\frac{4}{1+n}} \tag{11}$$

The estimated value of C for the base metal is 2.28 X 10^{15}. This value is lower than that experimentally determined, but it can still be considered as an approximate prediction.

FCI Threshold $(\Delta\sigma_{eqv})_{th}$

For a notched specimen of an ultra-high-strength steel, the maximum stress at the notch root is far lower than the yield stress when the equivalent stress amplitude is near the FCI threshold. Therefore, the maximum stress range, $\Delta\sigma$, at the notch root can be related to the nominal stress range, ΔS, in the following form:

$$\Delta\sigma = K_t \Delta S \tag{12}$$

According to the basic concept of the local stress-strain approach, no crack initiates at the notch tip if the local stress range at the notch tip is equal to or less than the endurance limit of the material $\Delta\sigma_c$ (Refs. 5, 6, 13):

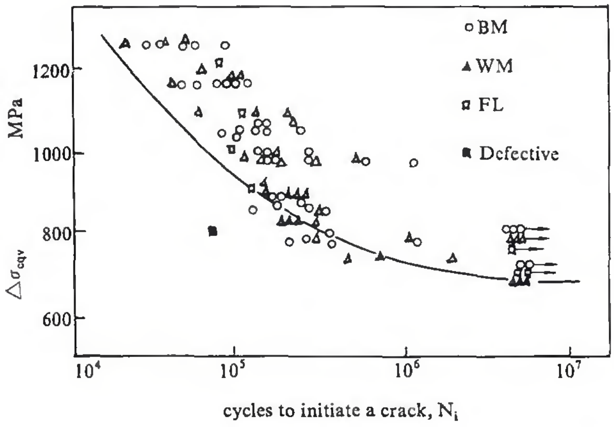

Fig. 5 — Comparison between the test data and the predicted curve of the FCI life.

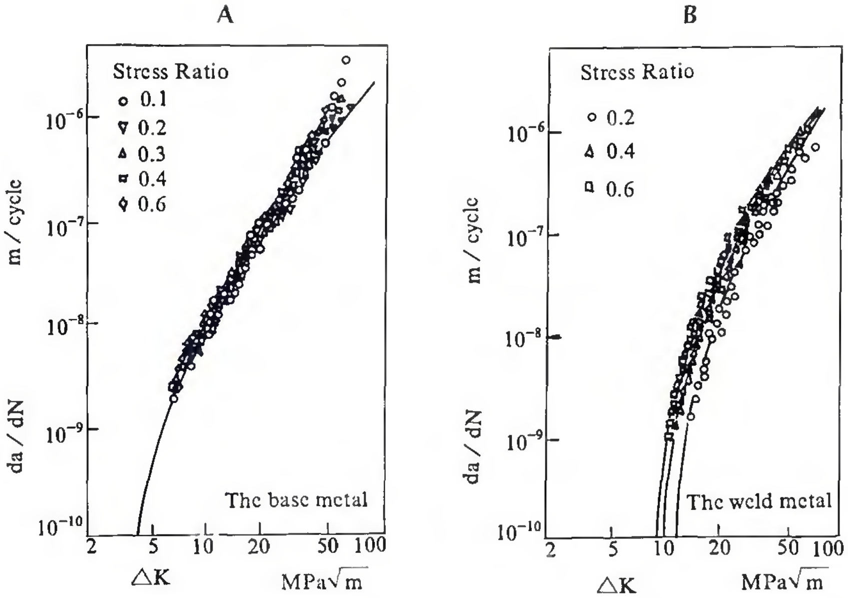

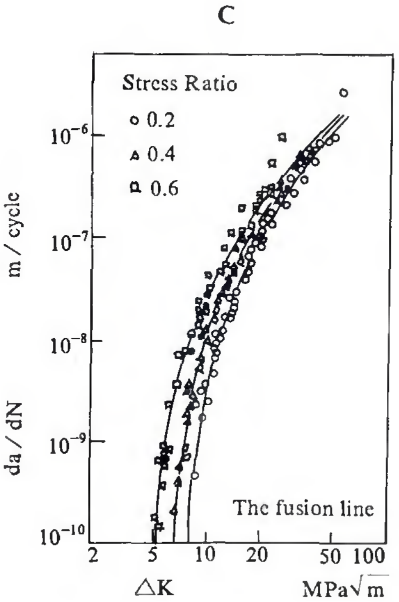

Fig. 6 — The test data and the least-squares fit curves of the FCP rates in different zones of the groove welds on 30Cr-Mn-Si-Ni-2A steel.

Table 3 — Analysis of the FCP Rate Test Results

Material	R	B MPa^{-2}	ΔK_{th} $MPa\sqrt{m}$	ΔK_{thE} $MPa\sqrt{m}$	ΔK_{thC} $MPa\sqrt{m}$	r[a]	s[a]
Base metal	0.1	2.00×10^{-10}	3.29			0.994	0.053
	0.2	2.28×10^{-10}	3.21			0.991	0.068
	0.3	3.62×10^{-10}	3.27			0.990	0.070
	0.4	3.05×10^{-10}	3.45			0.994	0.053
	0.6	3.61×10^{-10}	3.50			0.996	0.045
weld metal	0.2	2.26×10^{-10}	10.34			0.973	0.069
	0.4	4.43×10^{-10}	9.26			0.973	0.100
	0.6	4.13×10^{-10}	8.42			0.969	0.053
Weld interface	0.2	6.76×10^{-10}	7.39	7.88	8.05	0.967	0.196
	0.4	9.22×10^{-10}	6.20	6.78	6.77	0.902	0.346
	0.6	8.89×10^{-10}	5.12	5.51	5.70	0.969	0.228

(a) r – the correlation coefficient; s – the standard deviation.

$$\Delta\sigma \le \Delta\sigma_c \tag{13}$$

The endurance limit under different stress ratios can be correlated as follows (Ref. 25):

$$\sqrt{\frac{1}{2(1-R)}}\Delta\sigma_c = \sigma_{-1} \tag{14}$$

here σ_{-1} is defined as the maximum stress amplitude when the fatigue life of smooth specimens tends to infinity under fully reversed loads (R = –1). By taking $\Delta\sigma = K_t\Delta\sigma = \Delta\sigma_C$ and incorporating Equation 14 into Equation 6, we have

The endurance limit of steels can be

$$(\Delta\sigma_{eqv})_{th} = \sigma_{-1} \tag{15}$$

estimated by using the following empirical expression (Ref. 26):

The values of σ_{-1} estimated from Equa-

$$\sigma_{-1} = 0.39\sigma_b + \psi \tag{16}$$

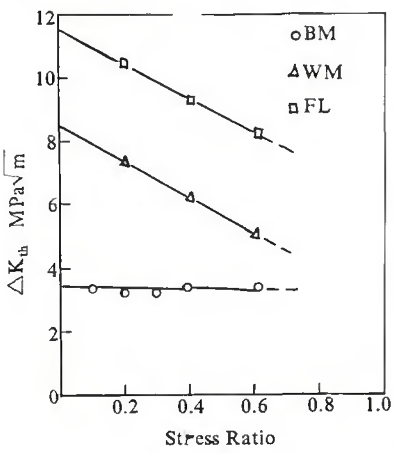

Fig. 7 — The correlation between ΔK_{th} and stress ratio R.

$$\sigma_{-1} + 0.41\sigma_b + \delta \tag{17}$$

tions 16 and 17 are 669 and 663 MPa (97 and 96 ksi), respectively. They agree well with the FCI threshold given in Equation 9a.

Prediction of FCI Life

According to the discussion above, the FCI life of the groove welds investigated can be approximately predicted by using the following equation:

Figure 5 shows Equation 18 can pre-

$$N_i = 0.25(0.1E)^{\frac{4}{1+n}}\left[\Delta\sigma_{eqv}^{\frac{2}{1+n}} - \sigma_{-1}^{\frac{2}{1+n}}\right]^{-2} \tag{18}$$

dict well the FCI life, but the predicted curve is slightly on the low side of the test data at the h gh equivalent stress amplitude because of the lower C value.

The FCP Test Results

The experimental results, e.g., in Refs. 14, 17, 27, show that the following equation gives a good fit to the test data on the FCP rate in metals:

where B is the FCP coefficient and ΔK_{th}

$$\frac{da}{dN} = B(\Delta K - \Delta K_{th})^2 \tag{19}$$

is the FCP threshold. The values of B and ΔK_{th} can be determined by processing the FCP data with the regression analysis method given in Ref. 14. The analysis results are listed in Table 3. Figure 6 presents the least-square fits to the test data. Substituting the values of B and ΔK_{th} into Equation 19, we can obtain the expressions of the FCP rates under different stress ratios.

Discussion of the FCP Test Results

FCP Coefficient B

The fractographs (Ref. 20) show that the striation crack growth mechanism operates within the intermediate region of the FCP (da/dN ≈ 10^{-8} to 10^{-6}m/cycle) in 30CrMnSiNi2A steel. In this case, the values of B can be predicted by using the following expression (Refs. 1, 4, 17, 27):

$$B = \frac{15.9}{E^2} \tag{20}$$

The value of B thus predicted is 3.75 X 10^{-10}MPa^{-2}. It is in reasonable agreement with the values of B experimentally determined for the base metal and the weld metal, but it is lower than those for the weld interface. The reason for this may be that a brittle FCP mechanism operates in the weld interface, so that the B values predicted from Equation 18 are lower than experimentally determined (Refs. 14, 17).

FCP threshold ΔK_{th}

The FCP thresholds of the weld interface experimentally determined, ΔK_{thE}, are higher than those of ΔK_{th} as shown in Table 3. This is reasonable due to their definitions. The former is the value of ΔK when da/dN = 3 X 10^{-10}m/cycle, while the latter is the maximum ΔK value below which the fatigue crack stops propagating. In order to make a comparison on the same basis, the ΔK values at da/dN = 3 X 10^{-10} m/cycle, denoted as ΔK_{thC}, are calculated by substituting the values of B and ΔK_{th} into Equation 17. As indicated in Table 3, the values of ΔK_{thE} and ΔK_{thC} are in good agreement.

The test results in Fig. 7 show that the FCP thresholds of the weld metal and the weld interface decrease linearly with an increasing stress ratio, but those of the base metal are independent of the stress ratio. The stress ratio independence of ΔK_{th} in the base metal may be due to the flat appearance of the fracture surface, which greatly reduces the crack closure effect (Ref. 28). The best fits to the correlation between the ΔK_{th} and R are as follows:

for the base metal

$$\Delta K_{th} = 3.34\ MPa\sqrt{m} \tag{21a}$$

for the weld metal

$$\Delta K_{th} = 11.26 - 4.8R\ MPa\sqrt{m} \tag{21b}$$

for the weld interface

$$\Delta K_{th} = 8.51 - 5.7R \; MPa\sqrt{m} \qquad (21c)$$
$$0 \le R \le 0.6$$

The General Expressions for the FCP Rates

By substituting Equations 18 and 19 for Equation 17, the general expressions for the different zones in the groove welds investigated are as follows:

for the base metal

$$\frac{da}{dN} = 3.75 \times 10^{-10}[\Delta K - 3.34]^2 \qquad (22a)$$

for the weld metal

$$\frac{da}{dN} = 3.75 \times 10^{-10}[\Delta K - (11.26 - 4.8R)]^2 \qquad (22b)$$

for the weld interface

$$\frac{da}{dN} = 9.00 \times 10^{-10}[\Delta K - (8.51 - 5.7R)]^2 \qquad (22c)$$
$$0 \le R \le 0.6$$

Application of Fatigue Tests Results

The analytical and experimental results (Ref. 4) indicate that the true stress concentration factor K_t at the weld toe of the welds investigated is about 3.5 and the K_t produced by a single cavity is about 2.2 to 2.8 (Ref. 22). So, fatigue cracks are likely to initiate at the weld toe if the weld reinforcement is not machined off. In this case, a discontinuity at the surface of the weld toe, such as undercut, will reduce the FCI life, but the inner noncrack-like discontinuities, such as cavities, have little effect on the FCI resistance. When the stress concentration at the weld toe is eliminated by removing the weld reinforcement, the FCI resistance will be improved, but the weld discontinuities or other discontinuities at the free surface may become FCI locations (Ref. 4). Since the strength of the base metal is greater than the weld metal, the FCI resistance of the base metal is more sensitive to welding discontinuities and surface conditions (Ref. 29). Note that the FCI life data in the present study were obtained from the specimens with a ground surface at the notch root. In structural life prediction, not only the effect of stress concentration produced by the geometry of the welded component, but also the influence of the undercut and difference in surface conditions on the FCI life have to be taken into account, otherwise a prediction will be given on the unsafe side, especially at low cyclic stress level (Refs. 1, 30).

The crack propagates initially in the HAZ, the weld metal or the base metal depending on the FCI locations. The results previously stated indicate the microstructure has a great effect on the FCP in the near-threshold region. In order to predict the fatigue life of welded components more accurately, the test results of FCP rate selected should be reasonably in line with the real FCI location and FCP path. The FCP life prediction will be on the safe side if the test results of the base metal or Equation 20a are used.

Conclusions

1) The postweld isothermal quenching treatment improves both the microstructure and the fatigue resistance of the groove welds on 30CrMnSiNi2A steel.

2) There is little difference in the FCI life of various zones in the groove welds. The general expression for the FCI life of the groove welds is as follows:

$$N_i = 6.48 \times 10^{15}\left[\Delta\sigma_{eqv}^{\;1.85} - 648^{1.85}\right]^{-2}$$

3) The following expression can be used to approximately predict the FCI life of the welds investigated:

$$N_i = 0.25(0.1E)^{\frac{4}{1+n}}\left[\Delta\sigma_{eqv}^{\frac{2}{1+n}} - \sigma_{-1}^{\frac{2}{1+n}}\right]^{-2}$$

4) The expressions for the FCP rates in the different zones of the groove welds are as follows:

for the base metal:

$$\frac{da}{dN} = 3.75 \times 10^{-10}[\Delta K - 3.34]^2$$

for the weld metal:

$$\frac{da}{dN} = 3.75 \times 10^{-10}[\Delta K - (11.26 - 4.8R)]^2$$

for the weld interface

$$\frac{da}{dN} = 9.00 \times 10^{-10}[\Delta K - (8.51 - 5.7R)]^2$$
$$0 \le R \le 0.6$$

5) In structural life prediction, the effects of undercut and surface condition should be taken into account and the test results or expressions of the FCI life and the FCP rate should be properly selected. A prediction on the life of the welds investigated will be on the safe side if the fatigue test results of the base metal are used.

References

1. Zheng, X., Lü, B., Cui, T., Lü, X., and Shi, Y. 1991. Prediction of fatigue life of 16-Mn steel butt welds. *J. Northwestern Polytechnical University* 9(1): 21–29 (in Chinese).
2. Lawrence, F. V., Jr., and Mazumdav, P. K. 1979. Application of strain controlled fatigue concepts to the prediction of weldment fatigue life. *Proc. Int. Symp. Low-cycle Fatigue Strength and Elasto-plastic Behavior of Materials*, Stuttgart, Germany, pp. 469–478.
3. Zheng, X., and Cui, T. 1989. Life prediction of butt welds containing welding defect. *Eng. Fract. Mech.* 34(5/6):1005–1011.
4. Lü, B., and Zheng, X. 1992. Prediction of fatigue life for butt welds of 30Cr-Mn-Si-Ni-2A steel. Work to be published.
5. Coffin, J. F., Jr. 1978. Fatigue in machines and structures. *Fatigue and Microstructures*, , ASM International, Materials Park, Ohio, pp. 4–7.
6. Bhuyan, G., and Vosikovski, O. 1989. Prediction of fatigue crack initiation lives for welded plate T-joints based on the local stress-strain approach, *Int. J. Fatigue* 11(3): 153–160.
7. Bush, A. 1989. Prediction of fatigue life under aircraft loading with and without the material memory rules, *Int. J. Fatigue* 11(2): 97–106.
8. Forrnan, R. G. 1972. Study of fatigue crack initiation from flaws using fracture mechanics theory. *Eng. Fract. Mech.* 4: 333–345.
9. Maddox, S. J. 1974. Assessing the significance of flaws in welds subjected to fatigue. *Welding Journal* 15(9): 401-s to 409-s.
10. Lawrence, F. V., Jr., 1978. Estimation of fatigue crack propagation life in butt welds. *Welding Journal* 14(3): 212-s to 220-s.
11. Smith, I. F. C., and Smith, R. A. 1986. Measuring fatigue cracks in fillet welded joints. *Int. J. Fatigue*, 8(1): 41–45.
12. Ohta, A., Sasaki, E., Kosuge, M., and Nishijima, S. 1987. Fatigue Crack Growth and Threshold Stress Intensity Factor for Welded Joints, Current Japanese Materials Research, 1, Japanese Society of Mechanical Engineering, JSME, 181—200.
13. Zheng, X. Further study on fatigue crack initiation life — mechanical model for fatigue crack initiation. Int. J. Fatigue 8(1): 17–21.
14. Zheng, X., and Hirt, M. A. 1983. Fatigue crack propagation in steels. *Eng. Fract. Mech.*, 18(5): 965–974.
15. Leven, M. M., and Frocht, M. M. 1952. Stress concentration factors for single notch in flat bar in pure and central bending. *J. Appl. Mech.* 74(5): 560–561.
16. Mutoh, Y. 1981. On the equivalent thickness of a side-grooved specimen. *JSME Int., J.*, Ser. 1, 32(3): 432–438.
17. Lü, B., Lü, X., and Zheng, X. 1989. Effect of microstructure on fatigue crack initiation and propagation of 16Mn steel. *Metall Trans.*, 20A(3): 413–419.
18. Zheng, X., Lin, C., Jiang, H., and Lü, B. 1992. On Miner's Law. *Acta Aeronautica Sinica*, in press.
19. Zheng, X., Lin, C., and Zheng, 5. 1990. An approximate formula for calculating local strain range, advanced computational methods. *Proc. 1st Int. Conf. Localized Damage Computer Aided Assessment and Control*, ed.

M. H. Aliabadi, *et al.*, pp. 253–261.

20. Liu, J., and Huang, S. 1984. The relationship between morphology of martensite in medium carbon steels and fatigue crack initiation and growth. *Research on Strength of Metals*, The Press of Xi'an Jiaotong University, pp. 53–65 (in Chinese).

21. Hu, G. and Zhang, M. On the heat treatment improving strength and toughness of 30Cr-Mn-Si-Ni-2A steel. *Acta Aeronautica Sinica*, 11(12): B576–B581.

22. Masubuchi, K. 1980. Analysis of welded structures, residual stresses, distortion and their consequences. *International Series on Materials Science and Technology*, Vol. 33, Pergamon Press.

23. Zheng, X. 1985. Further study on fatigue crack initiation — life prediction of fatigue crack initiation life. *Proc. Conf. Fatigue Life*, ed. V. 5. Goel, ASM International, Materials Park, Ohio, pp. 1–4.

24. Zheng, X., and Qiao, S. 1981. The plastic deformation, microcrack initiation and fatigue crack initiation life of 30Cr-Mn-Si-Ni-2A high strength martensitic steel. *Recent Selected Papers of Northwestern Polytechnical University*, Part 1, AD-A 104327, pp. 220–238.

25. Zheng, X., and Lü, B. 1987. On a fatigue formula under stress cycling. Int. J. Fatigue 9(2): 169–174.

26. Lieurade, H. -P. 1981. *Fatigue of Materials and Structures*. The Press of Montreal University, pp. 31–70 (in French).

27. Zheng, X. 1987. A simple formula for fatigue crack propagation and a new method for the determination of ΔK_{th}. *Eng. Fract. Mech.*, 27(3): 465–475.

28. Rarichandran, K. S. 1987. Microstructural effects and crack closure during near threshold fatigue crack propagation in a high strength steel. *Metall. Trans.*, 18A(5): 865–876.

29. Duggan, T. V., and Byrne, J. 1977. *Fatigue as a Design Criterion*. The MacMillan Press Ltd., p. 11.

30. Lieurade, H. -P., and Maillard-Salin, C. 1980. Low cycle fatigue behavior of welded joint in high strength steels, *ASTM STP 770*, pp. 311–336.